Anodic vs cathodic potentiostatic control of a methane producing Microbial Electrolysis Cell aimed at biogas upgrading

Marco Zeppilli*, Paola Paiano, Marianna Villano, Mauro Majone

Department of Chemistry, Sapienza University of Rome, P.le Aldo Moro 5, 00185 Rome, Italy

*****Corresponding author

Phone: +39 0649913716; Fax: +39 06490631

Email address: marco.zeppilli@uniroma1.it

Abstract

A fully biological Microbial Electrolysis Cell (MEC) aimed at biogas upgrading has been operated under different operating conditions in order to enhance CO_2 removal from a synthetic biogas. Specifically, CO_2 reduction into CH_4 occurred at the MEC biocathode with the oxidation of organic substrates in the anodic chamber partially sustaining the energy demand of the process. In the cathode chamber, methane formation was the main driver of current generation which, in turn, sustained alkalinity generation and related CO_2 sorption. This study mainly focused on the minimization of the anodic and cathodic overpotentials to maximize the process efficiency. To accomplish this objective, an innovative strategy of MEC polarization was adopted, consisting in the shift of the potentiostatic control of the process from the anode (at + 0.2 V vs SHE) to the cathode (at -0.65, -0.90 and -1.00 V vs SHE), along with the control of the fluid dynamic conditions of the anode chamber. An almost complete (99%) energy recovery was obtained by methane production with the cathode potential controlled at -0.65 V vs SHE. Finally, at the MEC cathode, current was utilized to reduce CO_2 into CH_4 (with a cathodic capture efficiency of about 70%) as well as to promote CO_2 sorption into HCO_3^-. The latter represents the main CO_2 removal mechanism that accounted for 85% of the CO_2 removal.

Keywords: Microbial Electrolysis Cell; Biogas Upgrading; CO_2 removal; Reaction overpotential; Fluid dynamics effects

1 Introduction

Bioelectrochemical systems are innovative techniques that stand on the utilization of "electroactive" microorganisms as biocatalysts of electrochemical reactions. In particular, the ability of electroactive microorganisms to exchange electrons with a solid state electrode allowed the development of several bioelectrochemical devices with different applications in the environmental field, such as the electricity generation from wastewater treatment [1, 2], the removal of target pollutants [3-5], the production of target molecules [6, 7] or the desalinization of salty and brackish waters [8, 9]. As for the anodic side of bioelectrochemical systems, the ability of exoelectrogens microorganisms on the degradation of organic compounds has been widely explored in the last 20 years [10, 11], and the direct electron transfer from microbes to the electrode surface has been identified and characterized by the identification of specific c-type cytochromes or nanowire [12-14]. However, more recently, research on bioelectrochemical systems has been focused on the possibility to drive the cathodic reactions towards the production of target molecules by applying an external electric power [15, 16]. As an example, biocathodes can be exploited for the conversion of CO_2 into target molecules such as methane [17, 18] and short chain volatile fatty acids by using an appropriate inoculum and an electricity source [19, 20]. In this case, the bioelectrochemical system, commonly referred to as Microbial Electrolysis Cells (MEC) [21, 22], permits to couple CO_2 reduction to the generation of valuable products and the utilization of the surplus electricity energy production, giving the possibility to store part of the electrical energy into reduced chemical compounds such us hydrogen [23, 24], methane [25]or acetate [26]. In this frame, several authors recently focused their attention on the development of methane producing MEC, the so called bioelectromethanogenesis as an innovative strategy to couple CO_2 reutilization and the storage of the surplus electricity produced by renewable source [27, 28]. The proposed approached was recently named as Bioelectro Power-to-Gas approach (BPTG) [29, 30]. One of the main aspects of

BPTG is the availability, for the electromethanogenesis reaction, of concentrated gaseous streams of CO_2 from different industrial fields, and one of the most attractive CO_2-rich stream is represented by the biogas deriving from anaerobic digestion processes [31]. Biogas is a gas mixture mainly composed by methane and CO_2, which is typically utilized for the cogeneration of heat and electric power in stationary applications [32]. CO_2 removal from biogas, also named upgrading process, permits to obtain biomethane, which has the same characteristics of natural compressed gas (CNG) and it can be used in automotive engines or injected into the distribution grid [33, 34]. The possibility to use a biological approach [35], such as a methane producing MEC, as an innovative biogas upgrading approach has been proposed in the literature by several authors [36-38]. The integration of the anaerobic digestion with a methane producing MEC, has been widely proposed by several authors [39, 40], which proposed both in situ and ex situ combination of the two technology. Recently, the main CO_2 removal mechanisms in a biocathode have been identified, particularly the sorption of CO_2 in the catholyte plays a pivotal role since it that permits the removal of up to 9 moles of CO_2 for each mole of methane produced [41]. Indeed, the sorption mechanism is driven by the alkalinity generation in the cathodic chamber due to the ionic transport of different ionic species for the electroneutrality maintenance [42, 43]. In the present work, a fully bio-catalyzed microbial electrolysis cell has been deeply studied testing different previously unexplored operating conditions in order to evaluate its performance in terms of both CO_2 removal efficiency and energy efficiency. More in detail, the most innovative approach hereby proposed consists in the sequential polarization of the anodic and cathodic chamber of the MEC as a strategy to minimize the overall energy consumption [44]. Also, the anodic fluid dynamics conditions have been found to significantly affect the anode overpotentials and, as a consequence, the energy consumption of the overall process. Finally, three different cathodic potentials (i.e., -0.65, -0.90, and -1.0 V vs. the Standard Hydrogen Electrode) have been investigated to identify the best operating conditions

which allow to enhance the process performance, in terms of methane production and CO_2 removal, while simultaneously lowering the overall energy consumption.

2. Experimentals

2.1 Microbial electrolysis cell design and setup

The microbial electrolysis cell (MEC) here proposed consisted of two identical Plexiglas chambers bolted together between two Plexiglas plates [45]. The two chambers, representing the anodic and cathodic compartment, were characterized by an internal volume of 0.86 L and separated by a pretreated Fumasep FAD anion exchange membrane (AEM) (Figure 1).

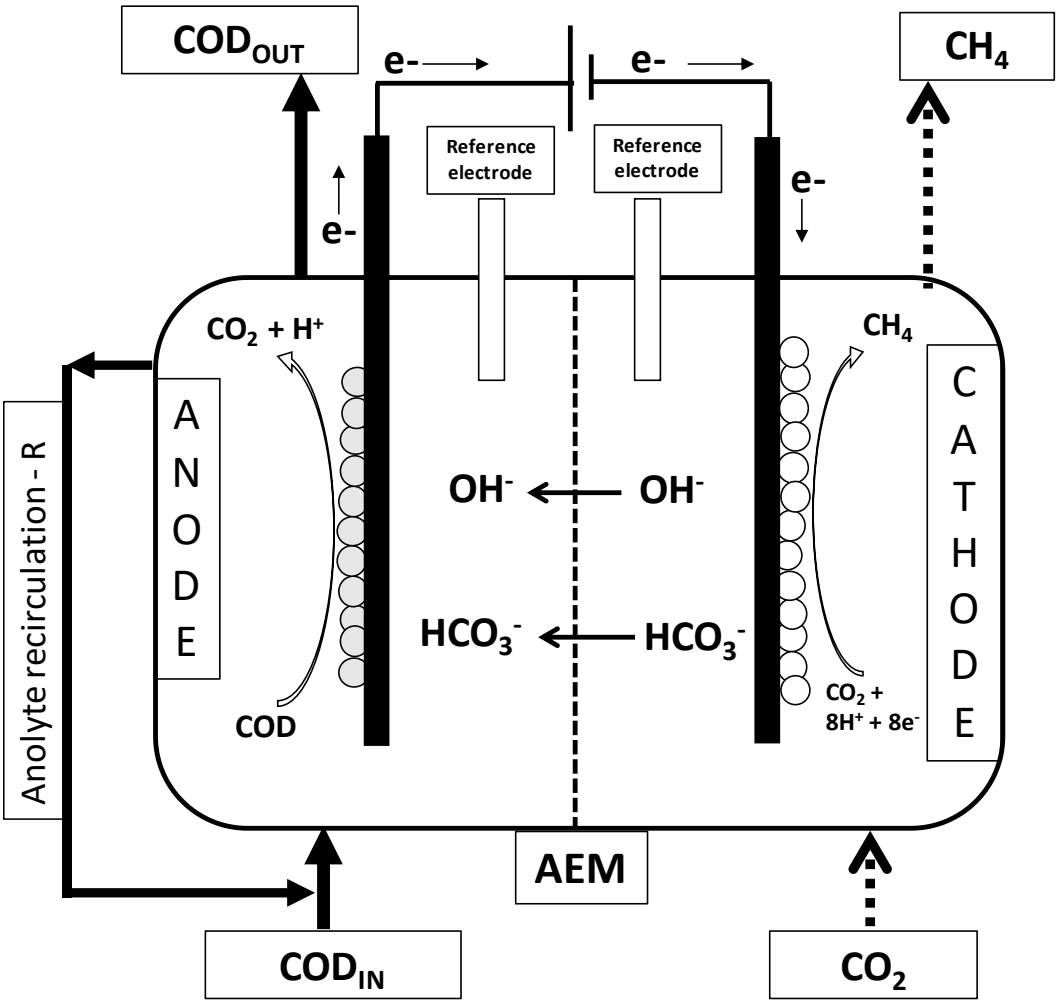

Figure 1: Scheme of the adopted Microbial Electrolysis Cell

Each MEC compartment was firstly filled with graphite granules, characterized by a diameter ranging from 2 to 6 mm (El Carb 100, Graphite Sales, Inc, USA), and previously treated to remove impurities from the surface [18]. In order to guarantee an external electrical connection, graphite rod

electrodes (5 mm diameter, Sigma–Aldrich, Italy) and Ag/AgCl reference electrode (+0.20 V vs. Standard Hydrogen Electrode, SHE) (Amel s.r.l., Milan, Italy) were placed in both electrodic chambers. For routine analyses of the gaseous and liquid phase, a sampling chamber was placed in the outlet of each compartment. In order to simulate the biogas composition (in terms of CO_2) deriving from anaerobic digestion processes, a N_2/CO_2 (70/30 %, v/v) gas mixture was continuously flushed into the cathodic chamber while the volumetric flow rate of the effluent gas phase was measured through a milliGas counter (Ritter, Germany). The liquid phase of the cathode was continuously recirculated at a flow rate of 60 mL/min and daily refilled with mineral medium to compensate the electroosmotic flux of solvent through the membrane from the cathodic to the anodic chamber. Using a fill and draw reactor, a hydrogenophilic community selection was made on the anaerobic sludge here used before inoculating it into the cathodic compartment of the MEC. On the anodic side, an activated sludge deriving from a full-scale wastewater treatment plant was used, which was maintained in absence of oxygen in order to use the electrode as electron acceptor for the oxidation of the organic matter. The latter consisted of a synthetic organic mixture continuously fed in the MEC anode and prepared as follows (g/L): peptone (0.138), yeast extract (0.075), sodium acetate (0.088), glucose (0.34) and also NH_4Cl (0.125), $MgCl_2$ $6H_2O$ (0.1), K_2HPO_4 (4.0), $CaCl_2{\cdot}2H_2O$ (0.05) as well as 10 mL/L of a trace metal solution [46] and 1 mL/L of vitamin solution [47]. The anodic liquid phase was recirculated at different flow rates through a peristaltic pump, thus, the ratio between the recirculation flow rate and the influent flow rate has been expressed as the recirculation factor (R) parameter expressed as:

$$\mathrm{R} = \frac{Q_{recirculation}}{Q_{influent}}$$

When the R resulted 0, i.e. no recirculation of the anolyte was present, the fluid dynamic condition of the anode chamber was named as “plug flow reactor (PFR)” while with a recirculation factor

higher than 10, the fluid dynamic condition of the anodic chamber was named as “continuous stirred tank reactor (CSTR)” condition.

Using a potentiostat (Bio-Logic), the MEC was operated with a 3-electrode configuration with the anode or the cathode functioning as the working electrode. During this start-up period, the anode constituted the working electrode and it was polarized at +0.20 V vs SHE using the Ag/AgCl reference electrode placed in the chamber. Subsequently, a shift in the potential control was operated, polarizing the cathode at three different cathodic potentials (-0.65 V, -0.90 and -1.00 V vs SHE), with the anode being the counter electrode. Throughout the paper, all of the potentials are reported against the Standard Hydrogen Electrode (SHE)

2.2 Electrochemical data collection and elaboration

The MEC was operated by a three-electrode configuration under either anodic or cathodic potentiostatic operation. The potentials of each chamber were detected by a multimeter with respect to the respective reference electrode and were named as $Ean_{(meas)}$ and $Ecath_{(meas)}$ for the anode and cathode chamber, respectively. The external applied voltage (ΔV) was determined by a multimeter that measured the voltage drop between anode and cathode electrodes. The ΔV in an electrolysis cell can be expressed as follows:

$$\Delta V = E_{cath(meas)} - E_{an(meas)} + \sum \eta$$

Where $\sum \eta$ represents the sum of the overpotentials that cause an additional energy loss in the system. The $\sum \eta$ is referred to the energy losses due to the migration and the convection of the ions for the electroneutrality maintenance and it depends on several parameters such as ionic conductivity and the fluid dynamics behavior.

According to the literature [48], by the measured anodic and cathodic average potentials (i.e. $E_{an(meas)}$ and $E_{cath(meas)}$), it is possible to calculate the overpotentials for the anodic (η_{an}) and cathodic (η_{cath}) reactions using the following expressions:

$$\eta_{an} = E_{an(meas)} - E_{an(eq)}$$

$$\eta_{cath} = E_{cath(meas)} - E_{cath(eq)}$$

where the equilibrium voltages for the anodic ($Ean_{(eq)}$) and cathodic ($Ecath_{(eq)}$) reactions are calculated according to the Nernst equation. As for the anodic oxidation reaction, the acetate oxidation was chosen due to previous experiments performed at same anodic conditions (i.e. same inoculum and same feeding solution), which had shown that the organic substrates were fermented into short chain VFA before being consumed by the anodophilic microorganisms[49]. Thus, the Nernst equation for the anodic reaction resulted:

$$2HCO_3^- + 8\,e^- + 9H^+ \rightarrow CH_3COO^- - + 2H_2O$$

$$E_{an\,(eq)} = E^0 + \frac{RT}{8F}\ln\frac{[HCO_3^-]^2 * [H^+]^9}{[CH_3COO^-]}$$

E^0 was 0.187 V and acetate, HCO_3^- and H^+ concentrations were the average values in the anodic effluent during the considered steady state period (the acetate concentration was assumed equal to the COD concentration).

For the reduction reaction, the proton reduction was chosen because, during the reactor operation, the average cathodic potential resulted more negative than the equilibrium potential under physiological condition ($E^{0'}$ = -0.41 V at pH = 7) in all explored conditions. The proton concentration was calculated from the average pH in the cathodic chamber for the considered period, while for the hydrogen partial pressure the value of 0.0001 atm was considered [50], which represents the

lower limit for hydrogenophilic methanogens activity and was chosen because, no hydrogen was detected in the cathodic chamber during all over the MEC operation.

$$2H^{+}+2\,e^{-}\ \rightarrow\ +H_2$$

$$E_{cath\,(eq)} = E^{0}\ + \frac{RT}{2F}\ln\frac{[H^{+}]^{2}}{[pH_2]}$$

2.3 Calculations

In order to assess the performance of the anodic and cathodic reactions, the reactions concerning COD removal and methane production have been compared with the average current flowing in the circuit. As reported in Table 1, the electrochemical efficiency of the reactions can be assessed for the anodic and cathodic side of the MEC.

Table 1. Main anodic and cathodic parameters of the MEC.

COD removed (mgCOD/d)	$\boldsymbol{COD_{removed} = F_{in} * COD_{in} - F_{out} * COD_{out}}$	- **COD_{in}** and **COD_{out}** (mg/L)*:* influent and effluent COD concentrations; - **F_{in}** and **F_{out} (L/d)**: influent and effluent flow rates in the anodic chamber.
Coulombic Efficiency (CE, %)	$\boldsymbol{CE = \frac{meq_i}{meq_{COD}}}$	- **meq_i**: cumulative electric charge transferred at the electrodes (integration of the current over time divided by Faraday's constant 96485 C/eq); - **meq_{COD}**: cumulative equivalents released from COD oxidation, calculated considering a conversion factor of 4 meq/32gO_2.
The methane production rate ($rCH_{4(eq)}$)	$\boldsymbol{rCH_{4(mmol)} = \frac{mmol_{CH4}}{d} * 8 = \frac{meq_{CH4}}{d}}$	- **$rCH_{4(mmol)}$** (mmol/d): daily moles of methane produced; - **8 meq/$mmol_{CH4}$**: conversion factor.

The Cathode Capture Efficiency (CCE, %)	$$CCE = \frac{meq_{CH4}}{meq_i}$$	- **meq$_{CH4}$**: cumulative equivalents of produced methane; - **meq$_i$**: cumulative equivalents deriving from current.

2.4 Inorganic carbon mass balance

The inorganic carbon mass balance has been evaluated considering both the CO_2 concentration in the different gaseous phases and the HCO_3^- concentration in the liquid phases of the reactor. The global and the cathode inorganic mass balance, reported in Table 2, have been used to evaluate the different CO_2 removal mechanisms involved in the process.

Table 2. Main parameters considered for the inorganic carbon mass balance and energy balance calculations.

Global inorganic carbon mass balance		
$$Qcat_{in} * CO_{2\,in} + F_{in-an} * HCO_3^- in + F_{in-cath} * HCO_3^- in = Qcat_{out} * (CO_{2\,out}) + rCH_{4\,(mmol)} + Qan * CO_{2\,an} + F_{out-an} * HCO_3^- out$$		
		- **Q (L/d):** volumetric flow rates of the gaseous streams; - **F (L/d):** volumetric flow rates of the liquid streams**;** - **CO_2**: inorganic carbon concentration of gas phase; - **HCO_3^-**: inorganic carbon concentration of liquid phase.
CO_2 daily removal, ΔCO_2 (mmol/d)	$$\Delta CO_2 = Qcat_{in} * CO_{2\,in} - Qcat_{out} * CO_{2\,out}$$	- **Qcat$_{in}$** and **Qcat$_{out}$ (L/d):** influent and effluent gas flow rate in and from the cathode chamber; - **CO_{2in}** and **CO_{2out} (mmol/L)**: CO_2 concentration in the influent and effluent gaseous streams.
- **Cathode Inorganic carbon mass balance**		

- $\Delta CO_2 = r_{CH4(mmol)} + HCO^-_{3(transf)}$
- r_{CH4} **(mmol/d)**: molar rate of methane production; - $HCO^-_{3(transf)}$**:** bicarbonate transfer rate from the cathode to the anode.

2.5 Energy balance

The energetic performance of the MEC has been assessed by the evaluation of both the energy efficiency (η_E), i.e. the energy theoretically recovered through the production of methane, and the energy supplied to the system (Table 3). The daily energy consumption (W_{IN}), was also considered during the energy performance evaluation for the single operations, i.e. the COD and CO_2 removal, calculated as the ratio between the energy consumption and the daily COD (kWh/kgCOD) and CO_2 (kWh/Nm^3CO_2) removed in the anode and in the cathode chamber, respectively. The molar amount of removed CO_2 was converted in volumetric unit under normal conditions (Pressure of 1 atm, Temperature of 0 °C). Furthermore, considering an efficiency of conversion of methane into electricity of 40 %, the net energy consumption for COD and CO_2 removal have been also evaluated.

Table 3. Main parameters for the energetic evaluation of the process.

- **Energetic evaluation of the process**		
Energy efficiency of the process (η_E)	$\eta E = \frac{W_{CH4}}{W_{IN}} * 100$	- W_{CH4}**:** energy recovered from produced methane; - W_{IN}**:** external energy supplied to the system.
W_{CH4}	$W_{CH4} = rCH_{4(mmol)} \times \Delta G_{CH4}$	- $r_{CH4(mmol)}$ **(mmol/d):** the amount of produced methane; - ΔG_{CH4} **(-0.818 KJ/mmol):** molar Gibbs free energy for methane combustion.
W_{IN}	$W_{IN} = \Delta V \times I$	- **ΔV:** average potential difference; - **I:** electric current flowing in the reactor.
kWh/kgCOD	$\frac{\mathbf{kWh}}{\mathbf{kgCOD}} = \frac{W_{IN}}{\mathbf{kgCOD}_{removed}}$	- W_{IN}**:** daily energy consumption; - $\mathbf{kgCOD}$**:** daily COD removal
kWh/Nm^3CO_2	$\frac{\mathbf{kWh}}{\mathbf{kgCOD}} = \frac{W_{IN}}{Nm^3\mathbf{CO_2}}$	- W_{IN}**:** daily energy consumption;

		- $\boldsymbol{Nm^3CO_2}$: daily CO_2 removal

2.6 Analytical methods

The headspace anode and cathode compartments of the MEC was periodically sampled using a gas-tight syringe and injecting 50 µL of gas sample into a Dani Master GC (Milan, Italy) gas chromatograph equipped with a thermal conductivity detector (TCD) for the analyses of CO_2 and H_2. The same amount of MEC headspace samples was also injected into a Varian (Lake Forest, CA, USA) 3400 gas-chromatograph for methane determination. The chemical oxygen demand (COD) content in the anodic influent and effluent streams was determined using a commercial COD cell test (Merck, Darmstadt, Germany) while the liquid samples for the determination of the concentration of the total and the inorganic carbon were analysed using a total carbon analyser (TOC-V CSN Shimadzu). Further details are reported elsewhere [49].

3 Results

3.1 MEC Start-up and potentiostatic control of the anode @+0.20 V *vs.* SHE

After the inoculation of the anodic and cathodic chambers, the anode was poised at + 0.20 V in order to promote the selection of electroactive microorganisms able to use graphite electrodes as electron acceptor to oxidize the organic matter. To enhance the electroactive-biomass growth, acetate was continuously fed in the anodic chamber and after 20 days of operation, the electroactivity of the biomass was shown by electricity production. During the start-up period, a hydraulic retention time (HRT) of 12 h was maintained while the volumetric organic load rate (OLR) was around 1 gCOD/Ld. During this period, the internal recirculation of the anodic liquid phase was maintained at values that ensured a recirculation ratio (i.e. the ratio between the internal recirculation and the feeding solution flow rate) higher than 10, ensuring a good mixing and minimizing possible mass transfer limitation. The start-up period was also characterized by the establishment of the methanogenic activity in the cathodic chamber.

After the start-up period, from day 68, the synthetic mixture of organic substrates was utilized to feed the anodic chamber at an average flow rate of 1.7 ± 0.1 L/d, corresponding to an HRT of 12 h and an OLR of 1.07 ± 0.07 gCOD/Ld. The current raised up to the average steady-state value of 101 ± 3 mA while the influent and effluent anodic COD concentrations were 541 ± 17 and 150 ± 20 mgCOD/L, respectively; corresponding to a daily COD removal of 691 ± 37 mgCOD/d (76% removal of influent OLR). By taking into account the average value of current (101 ± 3 mA), it resulted an average coulombic efficiency (CE) of 105 ± 9 %.

During this steady state period, the cathodic chamber of the MEC produced 56 ± 5 meq/d of methane ($rCH_{4(meq)}$) that corresponded to an average cathode capture efficiency (CCE) of 61 ± 5 %. The CO_2 removal from the cathodic chamber resulted on average 64 ± 9 mmolCO_2/d, while the

catholyte bicarbonate concentration raised the average value of 3.26 ± 0.05 gHCO_3^-/L, due to the CO_2 sorption promoted by the alkalinity generation in the cathodic chamber. The energy efficiency of the MEC, resulted on average 52 ± 5 %. The MEC operation required the establishment of an external voltage of -1.24 ± 0.04 V between the anode and the cathode chamber; while the anodic potential was controlled by the potentiostat at the value of +0.20 V, the average cathodic potential ($E_{cath(meas)}$) resulted on average -0.65 V .

Overall, with respect a previous study in which the anodic chamber was operated without the internal recirculation of the anolyte (referred to as PFR condition), the anodic performance of the MEC was enhanced by the presence of the internal recirculation of the anodic liquid phase (referred to as CSTR condition). Indeed, according with data reported in [41], the MEC run with the same operating conditions (i.e. same anionic exchange membrane, same feeding solution same and potentiostatic condition) but with no internal recirculation of the anodic liquid phase showed a lower current production, a lower COD removal and a lower coulombic efficiency. Data for both conditions of the MEC operation are reported in Table 4. This suggests that in the presence of recirculation the anodic reaction was affected by a mass transfer limitation of organic substrates from the bulk of the anodic chamber to the electroactive biofilm.

Table 4. Effect of the anodic fluid dynamics on the anodic performance of the MEC

Anodic Potential	**(Zeppilli et al. 2016) + 0.20 V vs SHE**	**This study + 0.20 V vs SHE**
Fluid dynamics condition	PFR	CSTR
COD removal (mgCOD/d)	610 ± 51	691 ± 37
COD removal (%)	78 ± 7	75 ± 10
Current (mA)	68 ± 7	101 ± 3
Coulombic efficiency (%)	80 ± 15	105 ± 9

3.2 Shift to the potentiostatic control of the cathode @-0.65 V *vs.* SHE

Subsequently, in order to evaluate the effect of controlling the potential of the cathodic reaction instead of controlling the anodic one, the cathode became the working electrode of the cell, and it was poised at the value of -0.65 V, i.e. the average value of the cathodic potential observed under the previous anodic potentiostatic condition at +0.20 V. The current signal changed sign and became negative, and quickly stabilized itself at an average value of -79 ± 2 mA (the change of the sign was due to the convention that the cathodic current is negative). The anodic COD removal was on average 660 ± 49 mgCOD/d that accounted for a coulombic efficiency of 86 ± 8 %. Both methane production rate and CO_2 removal were slightly lower than that observed with the potentiostatic control of the anode, with average values of 48 ± 2 meqCH_4/d and 42 ± 4 mmol CO_2/d, respectively. The average CCE for methane production remained similar to that previously observed with an average value of 68 ± 4%; suggesting that the slightly lower methane production was directly correlated to the lower current flowing in the circuit. The difference of potential between the anode and the cathode (ΔV) after the shift of the potential control to the cathode resulted on average -0.77 ± 0.03 V; significantly lower (around 40 %) with respect to the value of -1.24 ± 0.02 V obtained during the previous condition with the potentiostatic control of the anode. Thanks to the latter effect, the energy efficiency ηE resulted on average 99 % indicating a complete (theoretical) energy recovery from methane production.

The average anodic potential measured after the shift of the potential control to the cathode, resulted on average -0.06 V; whereas the overpotential of the anodic reaction (ηA) resulted 0.59 V. With the same approach, the overpotential of the cathodic reaction (ηC) resulted 0.34 V. During the previous condition of anodic potentiostatic control, the average overpotentials for the anodic and cathodic reactions resulted 0.84 and 0.38 V, respectively. Hence, the shift of the potentiostatic

control from the anode to the cathode permitted to reduce the ηA from 0.84 to 0.59, corresponding to a 30 % reduction; on the contrary the ηC didn't change significantly between the two conditions (overpotential of 0.38 V during the anodic control and an overpotential of 0.34 during the cathodic control).

The ηA reduction caused by the shift to the cathodic potentiostatic control was likely due to the spontaneous minimization of the potential of the anodic reaction that served as counter electrode in the three-electrode system. Notably, the anodic potential spontaneously reached by the anode (-0.06 V) was similar to the anodic potentiostatic condition at -0.1 V which was already used in previous research and was found to minimize the energy demand of the MEC [49, 50].

3.3 Anodic Fluid dynamics effects on MEC performances under cathodic potentiostatic control at -0.65 V vs SHE

To better characterize possible effects of the anodic fluid dynamics condition while the MEC is operated under the cathodic potentiostatic control at -0.65 V, the recirculation ratio in the anodic chamber has been varied between 0 and 10. In figure 2 the relationships between R and ΔV (i.e., the difference of potential established between the cathode and the anode) (Figure 2-A) and between R and the anodic and cathodic potential (Figure 2-B) are reported. Each fluid dynamics condition was maintained for at least 6 HRT in order to obtain a stable measure.

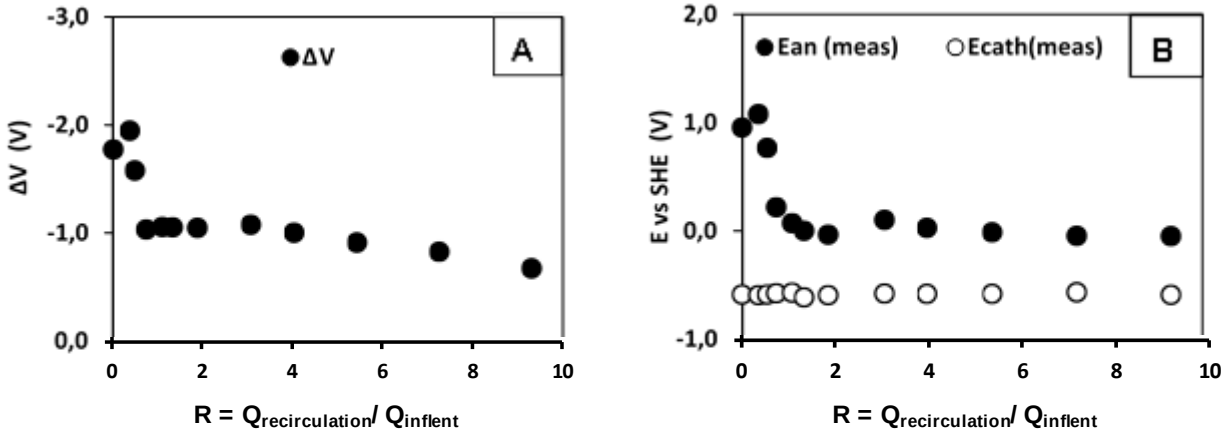

Figure 2. Correlation between the recirculation factor (R) and the overall ΔV (A) and between R and $E_{an(meas)}$ and $E_{cath(meas)}$ (B)

The removal of the internal recirculation of the liquid phase (named "PFR condition", recirculation ratio 0), resulted in a sharp increase of the potential difference between anode and cathode from -0.77 ± 0.03 to -1.76 ± 0.04 V. No significant changes in terms of current generation, COD oxidation and CH_4 production were observed during this PFR-like condition. The strong ΔV increase was also coupled to the increase of the anodic potential, that reached the value of + 0.96 V. As above mentioned, this was likely related to mass transport limitation of organic substrates involved in the anodic reaction from the bulk of the solution to the biofilm surface, that increased the anodic concentration overpotential. From Figure 2 it is evident that mass transfer resistance was controlling the process especially when the value of R was between 0 and around 1, to which corresponded a value of the anodic potential of 0.96 and -0.03 V, respectively. Moreover, according to figure 2-B, when the value of R was between 1 and 10, the anodic overpotential remained stable, indicating that even at a value of R of 1 the anodic turbulence was sufficient to minimize the mass transfer resistance of organic substrates from the bulk to the biofilm surface.

However, as showed in figure 2-A, the ΔV of the MEC showed a less sharp decrease for R higher than 2, that suggests that the further increase of the turbulence promoted additional mechanisms other

than the mass transport of the anodic substrates. By calculating the theoretical potential difference from the measured anodic and cathodic potential (figure 3-A)), it was possible to evaluate the energy loss due to the resistance of the electrolytes (figure 3-B) that depends on both the electrolyte composition and the fluid dynamics behavior.

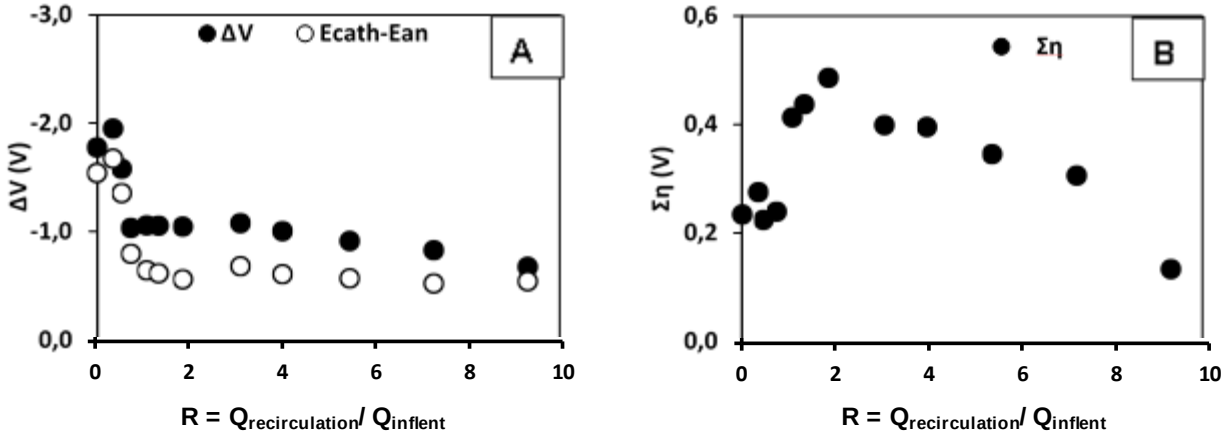

Figure 3. Theoretical and experimental potential difference (A) and ionic drop (B) as a function of the fluid dynamics behavior.

From a recirculation factor of 2 to 10, it was possible to observe a drop down from 0.49 to 0.13 V of the sum of overpotential. Hence, it is possible that from 0 to 2 the main resistance (overpotential) that influenced the overall ΔV was linked to the mass transfer of substrates involved in the anodic reaction, while from 2 to 10 the main resistance depended on the migration of ionic species involved in the electroneutrality maintenance. The latter parameter depends on several factors like the average distance between the electrodes and the anion exchange membrane, the conductivity of the electrolytes in the cathodic and anionic chamber and the mobility of the ionic species [42].

3.4 Control of the cathodic potential at -0.90 V vs SHE

By maintaining the anodic chamber at a value of R equal to 10, starting from day 146 the cathodic potential was poised at -0.90 V. The current sharply increased to higher values, that resulted on average -165 ± 4 mA (Figure 4) while the ΔV increased to the average value of -2.57 ± 0.06 V.

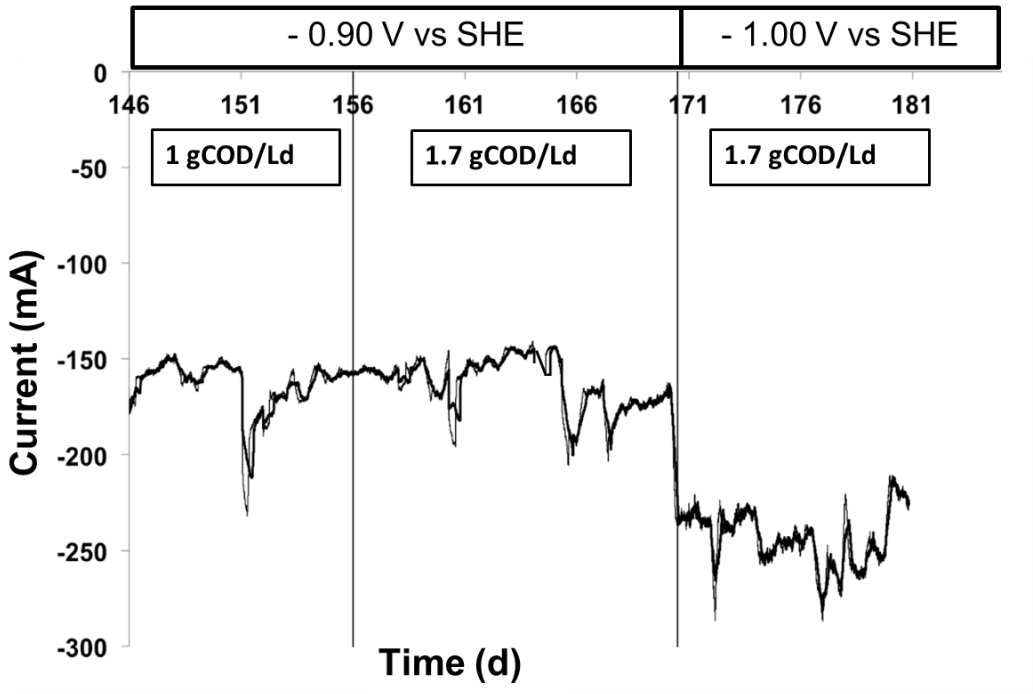

Figure 4. Time course of current during the two-different cathodic potentiostatic conditions

Under these conditions, the methane production rate increased to 110 ± 9 meq/d maintaining a stable CCE of 74 ± 5, while the CO_2 removal increased to an average value of 90 ± 10 mmol/d. Regarding the performance of the MEC anode, almost no COD concentration was detected in the anode outlet, resulting in a COD removal efficiency of 98 ± 3 %. The resulting CE for the anodic reaction accounted for 207 ± 14 %, indicating that the current flowing in the circuit was produced not only by the equivalents coming from COD oxidation, but also from other reactions such as water oxidation. The latter results were also confirmed by the measured anodic potential that resulted 0.97 V, a more oxidative potential with respect to the thermodynamic value (0.88 V) for water oxidation at pH 6.5 and low O_2 partial pressure (0.01 atm). Hence, to sustain the current production with the COD oxidation, the organic load rate to the anode chamber was almost doubled to supply

a non-limiting amount of organic carbon. As expected, after the increasing of the organic load rate to 1.7 ± 0.3 gCOD/Ld, the current profile did not significantly change, with an average value of -145 ± 4 mA. On the other hand, a daily removal of 1088 ± 73 mgCOD/d and an average CE of 98 ± 6 % were obtained. In this way, the equivalents supplied by the oxidation of organic substrates avoided water oxidation that produces molecular oxygen that could inhibit the cathodic methanogenic activity by oxygen diffusion. This is also in agreement with the fact that water oxidation typically requires higher potential values that that required the anodic COD oxidation and,. indeed, the anodic potential decreased from 0.97 V to 0.61 V. As for the cathode performance, as expected, methane production and CO_2 removal remained to value similar to the previous condition at an OLR of 1gCOD/Ld, of 93 ± 4 meq/d and 94 ± 8 mmol/d; respectively. The average ΔV established between the anode and cathode chamber resulted on average -2.35 ± 0.06 V and the energy efficiency resulted of 32 ± 4 %, a value higher (24%) than obtained with the lower OLR at the same cathode potential, but at the same time lower (99%) than the value obtained with the cathode potential controlled at -0.65 V.

3.5 Control of the cathodic potential at -1.0 V vs SHE

Starting from day 171 the cathodic potential was poised at -1.0 V. Under this condition, the current signal was particularly unstable and the average value accounted for -241 ± 54 mA. With a value of 1147± 108 mg/d of removed COD, that corresponded to a COD removal efficiency of 77± 20 %, it resulted an average CE of 151 ± 17 %. Unexpectedly, in the cathodic side of the MEC the methane production rate didn't increase, but remained at an average value of 86 ± 10 meq/d that also caused the drop down of the average CCE to 40 ± 5 %. On the other hand, during the -1.00 V condition, the CO_2 removal slightly increased to 102 ± 10 mmol/d, indicating that the methanogenic biofilm probably reached its maximum methane production rate and/or an inhibition effect of the applied

potential occurred. The -1.00 V was also characterized by the lowest energy efficiency, with an average value of 17 ± % that was caused by the higher applied voltage ΔV of - 3.01 ± 0.05 V between anode and cathode.

3.6 CO_2 removal and inorganic mass balance of the MEC

As also reported in previous experiments [41], the main CO_2 removal mechanism is the CO_2 sorption which is caused by the alkalinity generation in the cathodic chamber. The alkalinity generation is the direct effect on one side of the current and on the other side of the related transport of ions other than hydroxyl through the anion exchange membrane (that promotes a pH split between the anode and cathode chamber) [51]. As shown in figure 5, a direct correlation exists between the current flowing in the circuit and the CO_2 removal.

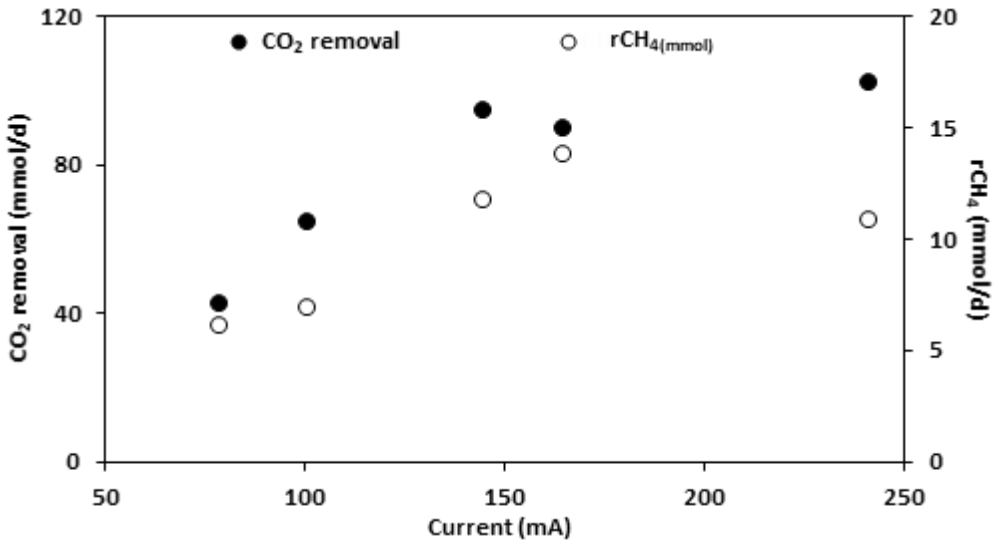

Figure 5. CO_2 removal (white dots) and methane production (black dots) as a function of the average current flowing in the MEC under the different applied potentiostatic conditions

This correlation can be easily explained by the presence of two CO_2 removal mechanisms, i.e. the methane production and the sorption of the CO_2 as HCO_3^- ion. Both mechanisms are correlated with

the average current, however their dependence on the current is different. Indeed, while CH_4 generation depends on the biocathode interphase kinetic (which typically involves the electrodic material, the reactants transport and the biofilm properties), the CO_2 sorption mainly depends on the electrolyte composition and the fluidynamic conditions of the anodic and cathodic liquid phase. Moreover, these two mechanisms are differently influenced by current also in terms of charge balance, because of the fact that 8 equivalents are required for CO_2 reduction into methane, whereas the migration of HCO_3^- (produced by CO_2 sorption) counterbalances only 1 equivalent of negative charge flowing through the cell circuit. This further supports the fact that the main CO_2 removal mechanism resulted in CO_2 sorption as HCO_3^-. The methane production at the highest value of current at -1.0 V slightly decreased from 14 to 11 mmol/d, on the contrary the CO_2 removal slightly increased from 90 to 100 mmol/d. This indicates that, independently from methane generation, the increase in the current can promote an increase in the alkalinity generation that permits a higher CO_2 removal.

Indeed, in figure 6, the time course of HCO_3^- concentration in the different MEC streams showed the increase of the cathodic HCO_3^- concentration promoted by the decrease of the applied cathodic potential. The average HCO_3^- concentrations recorded during the -0.65, -0.90 and -1.0 V potentiostatic conditions were 2.9 ± 0.1, 8.6 ± 0.3, and 9.3 ±0.5 gHCO_3^-/L, respectively.

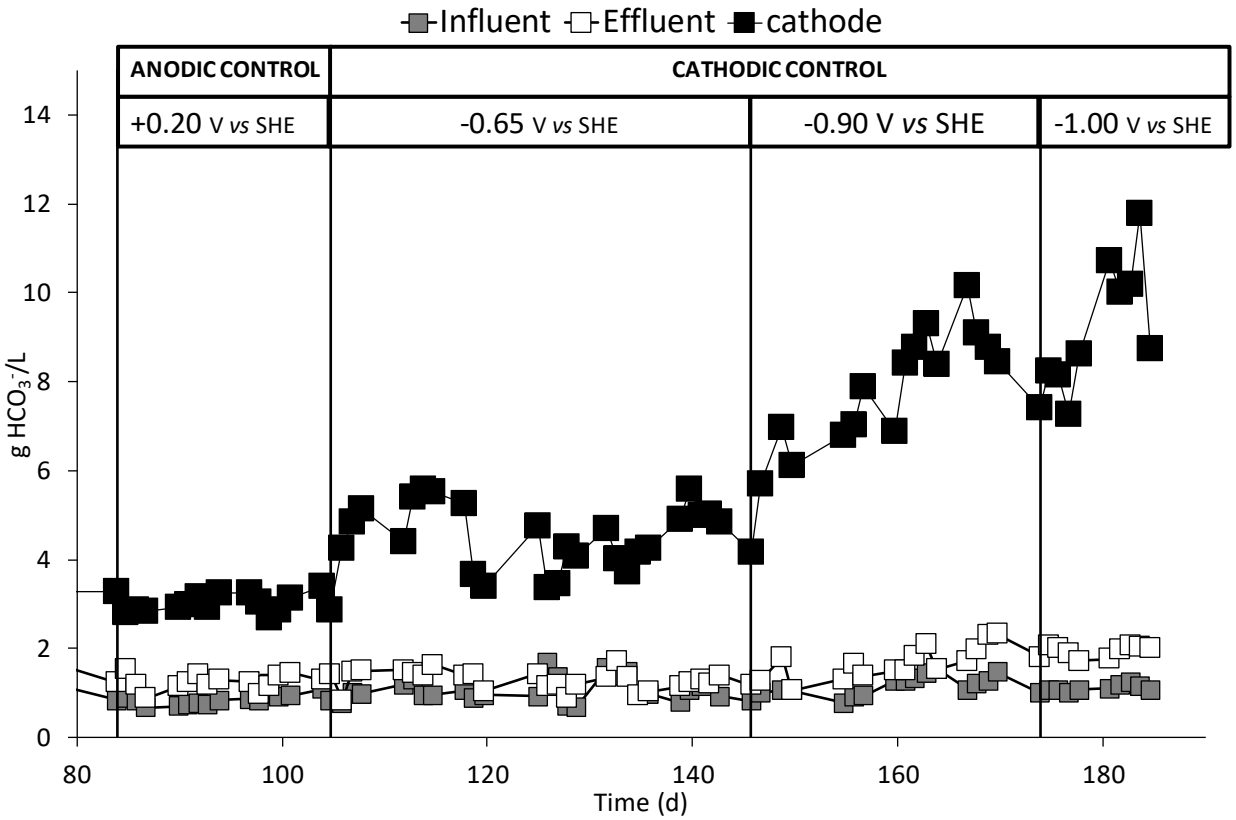

Figure 6. Time course of bicarbonate concentration in the different streams of the MEC.

The global inorganic carbon mass balance of the MEC (Table 5) permitted to assess the different transport and removal mechanisms involved in the CO_2 removal from the biocathode. Considering all the gaseous and liquid streams that contained inorganic carbon as CO_2 and HCO_3^-, respectively, it was possible to obtain an almost complete recovery of the outlet inorganic carbon with respect the inlet one.

Table 5. Inorganic carbon mass balance main results

Potential (V vs SHE)	**+ 0.2** (Anodic control) OLR 1 gCOD/Ld	**- 0.65** (Cathodic control OLR 1 gCOD/Ld)	**- 0.9** (Cathodic control) OLR 1 gCOD/Ld	**- 0.9** (Cathodic control) OLR 1.7 gCOD/Ld	**- 1.00** (Cathodic control) OLR 1.7 gCOD/Ld
ΔCO_2 (mmol/d)	64	42	90	94	102

rCH_4 (mmol/d)	7	6	12	14	11
HCO_3^- transferred (mmol/d)	57	36	83	79	88
HCO_3^- ionic transport (%)	63	50	50	61	40
IC balance recovery (%)	80	95	87	89	90

By the inorganic carbon mass balance was possible to underline that methane production contributed in a range between 10 and 15 % to the overall CO_2 removal that was mainly caused by the CO_2 sorption. The main CO_2 removal mechanism was the daily amount of HCO_3^- transferred from the cathode to the anode for the electroneutrality maintenance, that ranged from 36 to 88 mmol/d of removed CO_2 depending on the applied potential. On the other hand, because methane generation accounted for a significant part (CCE between 40 and 70 %) of flowing current it also contributed to alkalinity generation. It is also interesting that HCO_3^- migration through the anionic membrane accounted for the 40 to 63 % of the ionic current from the cathode to the anode chamber.

3.7 Energetic evaluation of the process

The energy efficiency of the process (ηE), that is the ratio between the energy recovered by the produced methane and the electrical energy consumed by the process, showed clearly that the more efficient explored condition was the one with the potentiostatic control of the cathode at -0.65 V and a recirculation ratio of the anodic liquid phase higher than 2. In this condition, an almost complete energy recovery (99%) was obtained; on the other hand, by increasing the cathodic potential at -0.90 and -1.00 V, the energy efficiency sharply decreased to 32 and 17 %, respectively.

The energy consumption for CO_2 removal was evaluated by considering the daily electrical energy utilized with respect the daily CO_2 removal in the cathodic chamber.

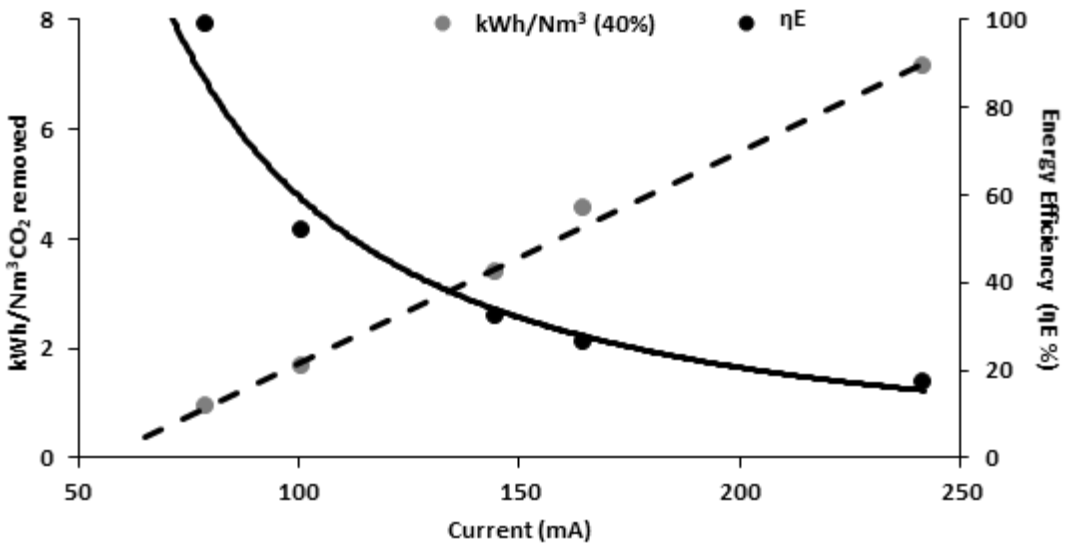

Figure.7: Energy consumption for CO_2 removal and energy efficiency as a function of the current flowing in the circuit.

In figure 7, both the energy consumption for CO_2 removal and the MEC energy efficiency as a function of the average current are reported. The energy consumption corresponds to the net energy consumption, that is calculated by also considering the electric energy which can be recovered by the methane produced (a yield of CH_4 conversion into electricity of 0.4 has been considered). The increasing of the current, promoted by the increasing of the cathodic potential, strongly increased the energy consumption to the CO_2 removal along with the decrease of the energy efficiency. In table 6, the main results regarding the energetic performances are summarized.

Table 6. Energetic parameters obtained during the different explored potentiostatic condition

Potential (V vs SHE)	**+ 0.2 (Anodic control)**	**- 0.65 (Cathodic control)**	**- 0.9 (Cathodic control)**	**- 1.00 (Cathodic control)**
ΔV (V)	-1.76	-0.77	-2.35	-3.01
I (mA)	101	79	145	241

kWh/Nm^{3}CO$_2$	2.09	1.55	3.87	7.65
ηE %	52	99	32	17
kWh/Nm^{3}CO$_2$ net	1.66	0.94	3.38	7.13

4 Conclusions

An MEC aimed at biogas upgrading has been operated for almost 200 days under a wide range of operating conditions. The analysis of the process performance in terms of CO_2 removal and energy efficiency, showed the possibility to minimize the energy consumption of an MEC aimed at biogas upgrading by both controlling the fluid dynamics of the anode chamber as well as shifting the potentiostatic control of the process form the anode to the cathode. The best condition in terms of energy efficiency resulted the potentiostatic control of the cathode at -0.65 V, which allowed a theoretical complete energy recovery. The increase of the cathodic potential at -0.90 V resulted in an increase of methane generation, whereas a possible inhibition of the cathodic biofilm was observed at a cathode potential of -1.0 V. Based on the obtained results, this study showed an innovative route for process optimization. Indeed, while the potentiostatic control of the anode resulted necessary for the start-up and the establishment of an electroactive biofilm, the shift of the potentiostatic control from the anode to the cathode allowed to maximize the energy efficiency of the overall process (from 52 to 99 %). Furthermore, this study showed a direct correlation between the current flowing in the MEC and the CO_2 removal in the cathodic chamber, in which the predominance of the CO_2 sorption due to the alkalinity generation accounted for the 80% of the removed CO_2. Finally, under the optimal explored condition (cathode potential at -0.65 V), the net energy consumption per unit of removed CO_2 accounted for 0.94 kWh/Nm^3CO_2, which is a value quite promising if compared to the present industrial technologies for biogas purification. This, along with the possibility to use cheap materials for electrodes and membranes, suggests the economic feasibility of the proposed technology.

Acknowledgments

This work has been carried out with the financial support of the project WE-MET "*Sustainable Wastewater treatment coupled to Energy recovery with Microbial Electrochemical Technologies"* (ERANET_NEXUS-14-035).

References

[1] B.E. Logan, B. Hamelers, R. Rozendal, U. Schroder, J. Keller, S. Freguia, P. Aelterman, W. Verstraete, K. Rabaey, Microbial fuel cells: methodology and technology, Environmental science & technology, 40 (2006) 5181-5192.

[2] H. Lin, W. Liu, X. Zhang, N. Williams, B. Hu, Microbial electrochemical septic tanks (MESTs): An alternative configuration with improved performance and minimal modifications on conventional septic systems, Biochemical Engineering Journal, 120 (2017) 146-156.

[3] F. Aulenta, R. Verdini, M. Zeppilli, G. Zanaroli, F. Fava, S. Rossetti, M. Majone, Electrochemical stimulation of microbial cis-dichloroethene (cis-DCE) oxidation by an ethene-assimilating culture, New Biotechnology, 30 (2013) 749-755.

[4] T. Hua, S. Li, F. Li, B.S. Ondon, Y. Liu, H. Wang, Degradation performance and microbial community analysis of microbial electrolysis cells for erythromycin wastewater treatment, Biochemical Engineering Journal, 146 (2019) 1-9.

[5] A. Arvin, M. Hosseini, M.M. Amin, G. Najafpour Darzi, Y. Ghasemi, A comparative study of the anaerobic baffled reactor and an integrated anaerobic baffled reactor and microbial electrolysis cell for treatment of petrochemical wastewater, Biochemical Engineering Journal, 144 (2019) 157-165.

[6] M. Zeppilli, I. Ceccarelli, M. Villano, M. Majone, Reduction of carbon dioxide into acetate in a fully biological microbial electrolysis cell, Chemical Engineering Transactions, 2016, pp. 445-450.

[7] M. Kuroda, T. Watanabe, CO2 reduction to methane and acetate using a bio-electro reactor with immobilized methanogens and homoacetogens on electrodes, Energy Conversion and Management, 36 (1995) 787-790.

[8] M. Zeppilli, A. Mattia, M. Villano, M. Majone, Three-chamber Bioelectrochemical System for Biogas Upgrading and Nutrient Recovery, Fuel Cells, 17 (2017) 593-600.

[9] X. Cao, X. Huang, P. Liang, K. Xiao, Y. Zhou, X. Zhang, B.E. Logan, A New Method for Water Desalination Using Microbial Desalination Cells, Environmental science & technology, 43 (2009) 7148-7152.

[10] B.E. Logan, Exoelectrogenic bacteria that power microbial fuel cells, Nature Reviews Microbiology, 7 (2009) 375.

[11] U. Schroder, Anodic electron transfer mechanisms in microbial fuel cells and their energy efficiency, Physical Chemistry Chemical Physics, 9 (2007) 2619-2629.

[12] Y.A. Gorby, S. Yanina, J.S. McLean, K.M. Rosso, D. Moyles, A. Dohnalkova, T.J. Beveridge, I.S. Chang, B.H. Kim, K.S. Kim, D.E. Culley, S.B. Reed, M.F. Romine, D.A. Saffarini, E.A. Hill, L. Shi, D.A. Elias, D.W. Kennedy, G. Pinchuk, K. Watanabe, S. Ishii, B. Logan, K.H. Nealson, J.K. Fredrickson, Electrically conductive bacterial nanowires produced by Shewanella oneidensis strain MR-1 and other microorganisms, Proceedings of the National Academy of Sciences of the United States of America, 103 (2006) 11358-11363.

[13] N.S. Malvankar, D.R. Lovley, Microbial nanowires for bioenergy applications, Current opinion in biotechnology, 27 (2014) 88-95.

[14] D.R. Lovley, Extracellular electron transfer: wires, capacitors, iron lungs, and more, Geobiology, 6 (2008) 225-231.

[15] B.E. Logan, D. Call, S. Cheng, H.V. Hamelers, T.H. Sleutels, A.W. Jeremiasse, R.A. Rozendal, Microbial electrolysis cells for high yield hydrogen gas production from organic matter, Environmental science & technology, 42 (2008) 8630-8640.

[16] D.F. Call, M.D. Merrill, B.E. Logan, High surface area stainless steel brushes as cathodes in microbial electrolysis cells, Environmental science & technology, 43 (2009) 2179-2183.

[17] S. Cheng, D. Xing, D.F. Call, B.E. Logan, Direct biological conversion of electrical current into methane by electromethanogenesis, Environmental Science and Technology, 43 (2009) 3953-3958.

[18] M. Villano, F. Aulenta, A. Giuliano, C. Ciucci , T. Ferri, M. Majone, Bioelectrochemical reduction of CO2 to CH4 via direct and indirect extracellular electron transfer by a hydrogenophilic methanogenic culture, Bioresource Technology, 101 (2010) 3085-3090.

[19] L. Jourdin, T. Grieger, J. Monetti, V. Flexer, S. Freguia, Y. Lu, J. Chen, M. Romano, G.G. Wallace, J. Keller, High Acetic Acid Production Rate Obtained by Microbial Electrosynthesis from Carbon Dioxide, Environmental science & technology, 49 (2015) 13566-13574.

[20] K.P. Nevin, T.L. Woodard, A.E. Franks, Z.M. Summers, D.R. Lovley, Microbial electrosynthesis: feeding microbes electricity to convert carbon dioxide and water to multicarbon extracellular organic compounds, mBio, 1 (2010).

[21] U. Schroder, F. Harnisch, L.T. Angenent, Microbial electrochemistry and technology: terminology and classification, Energy & Environmental Science, 8 (2015) 513-519.

[22] D.R. Lovley, K.P. Nevin, Electrobiocommodities: powering microbial production of fuels and commodity chemicals from carbon dioxide with electricity, Current opinion in biotechnology, 24 (2013) 385-390.

[23] Z. Huang, L. Lu, D. Jiang, D. Xing, Z.J. Ren, Electrochemical hythane production for renewable energy storage and biogas upgrading, Applied Energy, 187 (2017) 595-600.

[24] S. Luo, A. Jain, A. Aguilera, Z. He, Effective control of biohythane composition through operational strategies in an innovative microbial electrolysis cell, Applied Energy, 206 (2017) 879-886.

[25] R. Blasco-Gómez, P. Batlle-Vilanova, M. Villano, M. Balaguer, J. Colprim, S. Puig, On the Edge of Research and Technological Application: A Critical Review of Electromethanogenesis, International Journal of Molecular Sciences, 18 (2017) 874.

[26] D.R. Lovley, Powering microbes with electricity: Direct electron transfer from electrodes to microbes, Environmental Microbiology Reports, 3 (2011) 27-35.

[27] M.C.A.A. Van Eerten-Jansen, A.T. Heijne, C.J.N. Buisman, H.V.M. Hamelers, Microbial electrolysis cells for production of methane from CO2: long-term performance and perspectives, International Journal of Energy Research, 36 (2012) 809-819.

[28] L. Jürgensen, E.A. Ehimen, J. Born, J.B. Holm-Nielsen, Utilization of surplus electricity from wind power for dynamic biogas upgrading: Northern Germany case study, Biomass and Bioenergy, 66 (2014) 126-132.

[29] F. Geppert, D. Liu, M. van Eerten-Jansen, E. Weidner, C. Buisman, A. ter Heijne, Bioelectrochemical Power-to-Gas: State of the Art and Future Perspectives, Trends in biotechnology, 34 (2016) 879-894.

[30] X. Christodoulou, T. Okoroafor, S. Parry, S.B. Velasquez-Orta, The use of carbon dioxide in microbial electrosynthesis: Advancements, sustainability and economic feasibility, Journal of CO2 Utilization, 18 (2017) 390-399.

[31] M. Pöschl, S. Ward, P. Owende, Evaluation of energy efficiency of various biogas production and utilization pathways, Applied Energy, 87 (2010) 3305-3321.

[32] I. Bioenergy, Biomethane Status and Factors Affecting Market Development and Trade, (2014).

[33] E. Ryckebosch, M. Drouillon, H. Vervaeren, Techniques for transformation of biogas to biomethane, Biomass and Bioenergy, 35 (2011) 1633-1645.

[34] D. Andriani, A. Wresta, T.D. Atmaja, A. Saepudin, A review on optimization production and upgrading biogas through CO 2 removal using various techniques, Applied biochemistry and biotechnology, 172 (2014) 1909-1928.

[35] I. Angelidaki, L. Treu, P. Tsapekos, G. Luo, S. Campanaro, H. Wenzel, P.G. Kougias, Biogas upgrading and utilization: Current status and perspectives, Biotechnology Advances, 36 (2018) 452-466.

[36] P. Batlle-Vilanova, S. Puig, R. Gonzalez-Olmos, A. Vilajeliu-Pons, M.D. Balaguer, J. Colprim, Deciphering the electron transfer mechanisms for biogas upgrading to biomethane within a mixed culture biocathode, RSC Advances, 5 (2015) 52243-52251.

[37] H. Xu, K. Wang, D.E. Holmes, Bioelectrochemical removal of carbon dioxide (CO2): An innovative method for biogas upgrading, Bioresource Technology, 173 (2014) 392-398.

[38] A. Kokkoli, Y. Zhang, I. Angelidaki, Microbial electrochemical separation of CO2 for biogas upgrading, Bioresource Technology, 247 (2018) 380-386.

[39] Z. Yu, X. Leng, S. Zhao, J. Ji, T. Zhou, A. Khan, A. Kakde, P. Liu, X. Li, A review on the applications of microbial electrolysis cells in anaerobic digestion, Bioresource Technology, 255 (2018) 340-348.

[40] J. Park, B. Lee, D. Tian, H. Jun, Bioelectrochemical enhancement of methane production from highly concentrated food waste in a combined anaerobic digester and microbial electrolysis cell, Bioresource Technology, 247 (2018) 226-233.

[41] M. Zeppilli, A. Lai, M. Villano, M. Majone, Anion vs cation exchange membrane strongly affect mechanisms and yield of CO2 fixation in a microbial electrolysis cell, Chemical Engineering Journal, 304 (2016) 10-19.

[42] R.A. Rozendal, H.V. Hamelers, C.J. Buisman, Effects of membrane cation transport on pH and microbial fuel cell performance, Environmental science & technology, 40 (2006) 5206-5211.

[43] M. Oliot, S. Galier, H. Roux de Balmann, A. Bergel, Ion transport in microbial fuel cells: Key roles, theory and critical review, Applied Energy, 183 (2016) 1682-1704.

[44] M. Villano, G. Monaco, F. Aulenta, M. Majone, Electrochemically assisted methane production in a biofilm reactor, Journal of Power Sources, 196 (2011) 9467-9472.

[45] M. Villano, S. Scardala, F. Aulenta, M. Majone, Carbon and nitrogen removal and enhanced methane production in a microbial electrolysis cell, Bioresource Technology, 130 (2013) 366-371.

[46] W.E. Balch, G.E. Fox, L.J. Magrum, C.R. Woese, R.S. Wolfe, Methanogens: reevaluation of a unique biological group, Microbiological Reviews, 43 (1979) 260-296.

[47] J.G. Zeikus, The biology of methanogenic bacteria, Bacteriological Reviews, 41 (1977) 514-541.

[48] R.K. Thauer, K. Jungermann, K. Decker, Energy conservation in chemotrophic anaerobic bacteria, Bacteriological Reviews, 41 (1977) 100-180.

[49] M. Zeppilli, Villano M., Aulenta F., Lampis S., Vallini G., M. M., Effect of the anode feeding composition on the performance of a continuous-flow methane-producing microbial electrolysis cell, Environ Sci Pollut Res, (2014).

[50] M. Villano, C. Ralo, M. Zeppilli, F. Aulenta, M. Majone, Influence of the set anode potential on the performance and internal energy losses of a methane-producing microbial electrolysis cell, Bioelectrochemistry, 107 (2016) 1-6.

[51] T.H.J.A. Sleutels, H.V.M. Hamelers, R.A. Rozendal, C.J.N. Buisman, Ion transport resistance in Microbial Electrolysis Cells with anion and cation exchange membranes, International Journal of Hydrogen Energy, 34 (2009) 3612-3620.